

# Europium complex-based thermochromic sensor for integration in plastic optical fibres

Inma Suarez Lopez<sup>a</sup>, A. Luisa Mendonça<sup>b,c</sup>, Mariana Fernandes<sup>d</sup>, Verónica de Zea Bermudez<sup>d</sup>, Jorge Morgado<sup>b,c</sup>, G. Del Pozo<sup>e</sup>, B. Romero<sup>e</sup>, Juan Cabanillas-Gonzalez<sup>f,\*</sup>

<sup>a</sup> Dipartimento di Fisica, Politecnico di Milano, Piazza. Leonardo da Vinci 32, Milano 20133, Italy

<sup>b</sup> Instituto de Telecomunicações, Universidade Técnica de Lisboa, Av. Rovisco Pais, P-1049-001 Lisboa, Portugal

<sup>c</sup> Instituto Superior Técnico, Universidade Técnica de Lisboa, Av. Rovisco Pais, P-1049-001 Lisboa, Portugal

<sup>d</sup> Departamento de Química and CQ-VR, Universidade de Trás-os-Montes e Alto Douro, 5001-801 Vila Real, Portugal

<sup>e</sup> Departamento de Tecnología Electrónica, Universidad Rey Juan Carlos, calle Tulipán s/n, 28933 Móstoles, Spain

<sup>f</sup> Instituto Madrileño de Estudios Avanzados (IMDEA) en Nanociencia, Facultad de Ciencias, Av. Tomas y Valiente 7, Cantoblanco, 28049 Madrid, Spain

## ARTICLE INFO

### Article history:

Received 22 December 2011

Received in revised form 24 February 2012

Accepted 28 February 2012

Available online 31 March 2012

### Keywords:

Fluorescence

Thermochromism

Arrhenius

Europium

Sensors

## ABSTRACT

We report on a new thermochromic material containing a europium complex for thermal sensing through its fluorescence response to temperature. The ratio between the strong luminescence peak of europium (III) and a side band emission is employed as a new probe for optical sensing of temperature. The ratio is observed to follow an Arrhenius-type dependence with temperature. Based on these results we developed a thermal probe based on a segment of luminescent thermometer optically cemented to the tip of a PMMA fibre.

© 2012 Elsevier B.V. All rights reserved.

## 1. Introduction

The progressive shrinking of electronic and photonic devices from micron- to nano-scale size requires new diagnostics techniques compatible with spatial constraints. In particular, thermometry techniques require new approaches alternative to classical thermometers based on expansion/contraction of volume or thermoelectric properties, which are seriously limited in size resolution and accuracy [1]. For this purpose, nanosize thermocouples fabricated by lithography have been developed, being the spatial resolution determined by the geometric size of the thermocouple. Nevertheless, these sensors show some drawbacks such as that they provide only the temperature at the sensing module/device interface, they are subjected to electrical interference and diagnosis is limited in speed and data volume. One of the main strategies to provide local temperature in nanoscopic systems is the design of molecules and nanoparticles which exhibit a strong optical response to temperature. Nanomaterials for thermal sensing range from carbon nanotubes [2–5] to semiconducting quantum dots [6–10] nanostructured inorganic films, polymeric liquid

crystals, and thermochromic molecules. Optical probe of temperature has as main advantage the fact that it is insensitive to undesired electrical interference, allowing at the same time for advanced diagnosis, e.g. remote distance diagnosis by using optical fibres and simultaneous analysis on different local regions by multiplexing data acquisition. The type of optical probe employed to detect temperature is of diverse nature, from absorption/reflection, to Raman and Brillouin scattering, amplified spontaneous emission, as well as fluorescence measurements (steady state or transient).

In this work we address the use of europium complexes for thermal sensing through their fluorescence response to temperature. In general terms, fluorescent thermal probes rely on shift in emission spectrum, changes in the intensity and linewidth and variation on dynamics of emitting states. Each of these detection schemes has associated advantages and drawbacks. For instance, monitoring photoluminescence (PL) lifetime provides large sensitivity to temperature mainly due to the possibility to restrict detection to a temporal window where dynamics are thermally activated, excluding other temperature insensitive time domains. The disadvantage is that this detection method is unable to discriminate from additional decay channels that may arise from photodegradation or fluctuations in excitation intensity in the presence of non-linear emission behaviour. Analysis of time-integrated emission spectrum

\* Corresponding author.

E-mail address: [juan.cabanillas@imdea.org](mailto:juan.cabanillas@imdea.org) (J. Cabanillas-Gonzalez).

has on the other hand the advantage that its implementation is relatively simple and it allows for processing signals of larger magnitude, which is an advantage for remote sensing applications. Monitoring relative changes in intensity of two optical transitions from two thermally coupled energy levels is one of the most popular techniques for thermal sensing. When the difference in energy levels of two photoexcited states is comparable to the thermal energy, transitions between them are thermally activated. Thermally-induced changes in the population of states leads to a variation in the intensity ratio of the emission peaks, being an interesting principle for a thermometer. Moreover, fluctuations in laser excitation or bleaching effects do not influence the ratio values as far as thermal sensing transitions originate from a common primary excited state. Rare earth ions are excellent candidates for these applications owing to their energy level configuration, dominant radiative transitions rates, emission in the visible–near IR, and narrow linewidth emission together with moderate energy separation, which facilitates overlap-free spectral detection.

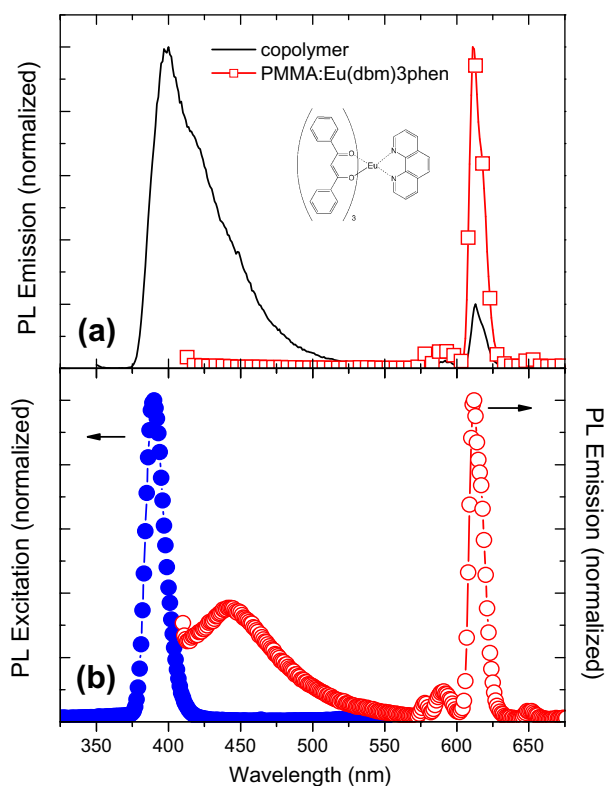
In this work we report on the strong thermochromism observed on a composite based on methylmethacrylate (MMA) and an  $\text{Eu}^{3+}$ -dibenzoylmethide ternary complex ( $\text{Eu}(\text{dbm})_3\text{phen}$ ), (chemical structure depicted in Fig. 1a). Upon excitation at 380 nm the material exhibits a dual emission composed of a temperature independent broad band at 450 nm and a strongly temperature dependent narrow emission peak at 612 nm attributed to the  $^5\text{D}_0 \rightarrow ^7\text{F}_2$   $\text{Eu}^{3+}$  electronic transition. The ratio between integrated photoluminescence (PL) values at both regions is thus strongly temperature dependent and constitutes the principle for a molecular thermometer.

## 2. Experimental

$\text{Eu}(\text{dbm})_3\text{phen}$  was prepared according to the procedure reported by Melby et al. [11] The composite was obtained by adding  $\text{Eu}(\text{dbm})_3\text{phen}$  to a glass test-tube containing methylmethacrylate (MMA) in a 0.03% total weight ratio in the presence of a catalytic amount of lauroyl peroxide. The solution test-tube was then placed in an oil bath at 60 °C for 140 min. At the end, the glass test-tube was broken to release the glassy rod of  $\text{Eu}(\text{dbm})_3\text{phen}$ -doped PMMA. For reasons discussed below, this  $\text{Eu}(\text{dbm})_3\text{phen}$ -doped PMMA material will be designated as *copolymer* in the following, as its properties are different from those corresponding to a simple mixture of PMMA and  $\text{Eu}(\text{dbm})_3\text{phen}$ . Samples for PL measurements consisted of slides of approximately 1 mm thickness cut from the main copolymer block and polished on both sides in order to make them optically accessible. PL measurements at various temperatures were performed with a Fluorolog fluorometer by fixing the slides to the cold finger of an Oxford Instruments cryostat. Measurements were performed in vacuum at approximately  $10^{-3}$  mbar. In order to enhance thermal contact between the slide and the cryostat finger a heat sink paste purchased from RS electronics was applied between the slide edge and the finger. PL acquisition was only started 10 min after the thermocouple reached each of the desired temperatures in order to favour thermalization of the copolymer slide. For measurements in plastic optical fibre (POF) a slide was fixed to the polished end of a single index PMMA fibre (radius 1 mm, length 3 cm) by using BC-600 Optical Cement from Saint Gobain Crystals and Detectors with matched refractive index to PMMA. Excitation in the UV was provided by an Omicron 375 nm 10 mW output laser. Detection was performed using a fibre coupled Ocean Optics spectrometer.

## 3. Results and discussion

The PL spectra of a copolymer slide and a spincoated blend film of  $\text{Eu}(\text{dbm})_3\text{phen}$  in PMMA with same  $\text{Eu}(\text{dbm})_3\text{phen}$  weight



content as the copolymer are compared in Fig. 1a. Upon excitation at 330 nm the emission spectrum of PMMA: $\text{Eu}(\text{dbm})_3\text{phen}$  blend exhibits the characteristic emission of  $\text{Eu}^{3+}$  with a dominant emission peak at 613 nm attributed to the  $^5\text{D}_0 \rightarrow ^7\text{F}_2$  electronic transition. No residual emission from dibenzoylmethide or phenanthroline ligands is observed, thus suggesting a complete energy transfer from the sensitizing ligands to  $\text{Eu}^{3+}$ . In this most general case, the  $\text{Eu}^{3+}$  emission occurs via an efficiently tailored energy transfer process [12–14] comprising (i) light absorption by the ligands, (ii) efficient intersystem crossing from the singlet to the triplet manifold of the ligands and (iii) energy transfer to  $\text{Eu}^{3+}$  ion followed by subsequent radiative decay. Based on this principle, efficient OLEDs were fabricated employing blends of conjugated polymer and Eu-complexes as emissive layer, involving an efficient Forster transfer from the host polymer to the ligands of the Eu-complex. [15]

In contrast, the PL spectrum of the copolymer displays two contributions: a dominant band with peak at 395 nm, ascribed to residual emission from the ligands, and less intense  $\text{Eu}^{3+}$  emission. Furthermore, the PL excitation spectrum of copolymer detecting at 613 nm (Fig. 1b) depicts a dominant peak at 390 nm coincident with the  $^7\text{F}_0 \rightarrow ^5\text{L}_6$  electronic transition in  $\text{Eu}^{3+}$ , indicating that emission in copolymer occurs predominantly via direct excitation of the  $\text{Eu}^{3+}$  ion. This result is in clear contrast with the PL excitation spectrum reported in  $\text{Eu}(\text{dbm})_3\text{phen}$  by Huang et al. [16] which displays intense broad bands due to sensitization of both dibenzoylmethide (in the UV-blue spectral range) and phenanthroline (deep UV spectral range) moieties. We thus believe that breaking of the  $\text{Eu}^{3+}$ –ligand coordination bonds during the MMA polymerization reaction process could partially hindered the  $\text{Eu}^{3+}$  ion antenna effect. It is worth noting that  $\text{Eu}^{3+}$  emission disappears when the copolymer block is dissolved in toluene. Only ligand

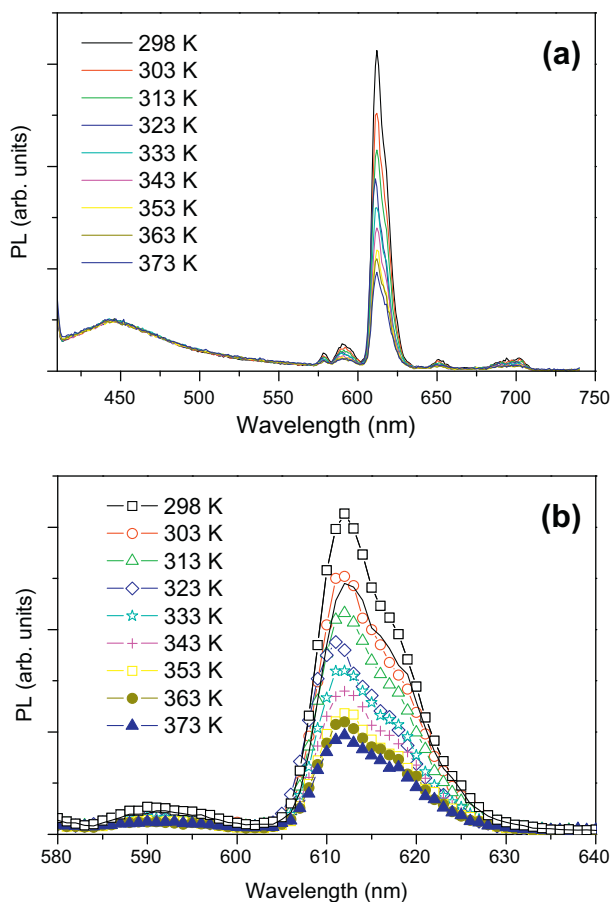


**Fig. 2.** (a) Reduction of  $\text{Eu}^{3+}$  emission from copolymer as the temperature is increased from 300 to 373 K. Each spectrum was normalized at the maximum of the blue band. (b) Same spectrum re-scaled.

emission is observed in the resulting solution or a spincoated film prepared from the solution. Though the exact mechanism is not yet known, we believe that the dbm ligand which sensitizes  $\text{Eu}^{3+}$  loses its coordination [17] in the presence of the radicals of the growing PMMA chains. Interestingly, energy transfer to  $\text{Eu}^{3+}$  ions in copolymer is retained to some extent as shown in Fig. 1a. Partial sensitization of the polymer is probably related to the increased viscosity during polymerization which leads to a glassy PMMA ( $T_g = 120^\circ\text{C}$ ), where the dbm ligands remain in close vicinity of the  $\text{Eu}^{3+}$  ion, thus retaining some sensitization ability. This *cage effect* is lost when the copolymer is dissolved and the dbm ligand (or some modification of it after reaction with the growing MMA chain) is dispersed in solution. We have also observed that upon heating a solution of  $\text{Eu}(\text{dbm})_3\text{phen}$  in MMA for 7 h at  $65^\circ\text{C}$  (the MMA polymerization temperature) without initiator to avoid MMA polymerisation, no residual ligand emission nor quenching of  $\text{Eu}^{3+}$  emission are observed, ruling out the simple temperature effect. Only when MMA polymerisation is carried out in the presence of  $\text{Eu}(\text{dbm})_3\text{phen}$ , both significant residual ligand emission and  $\text{Eu}^{3+}$  emission quenching are visible. Based on these conclusions we infer that emission of copolymer upon 380 nm excitation (Fig. 1b) is likely the result of direct excitation into europium ion levels and of energy transfer from dbm ligands to much less extent. The blue<sup>1</sup> emission band likely arises from residual dbm emission. Note that alternative explanations such as the formation of a new

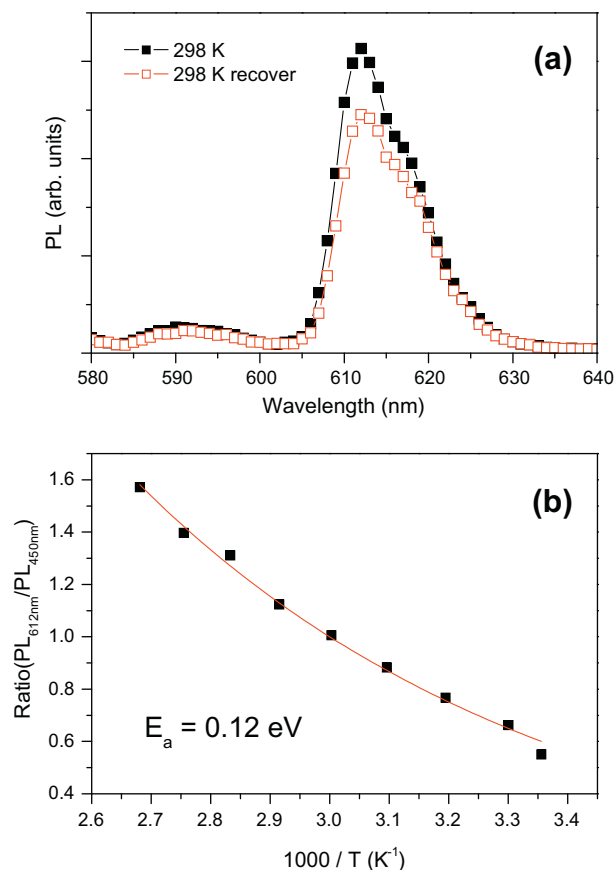
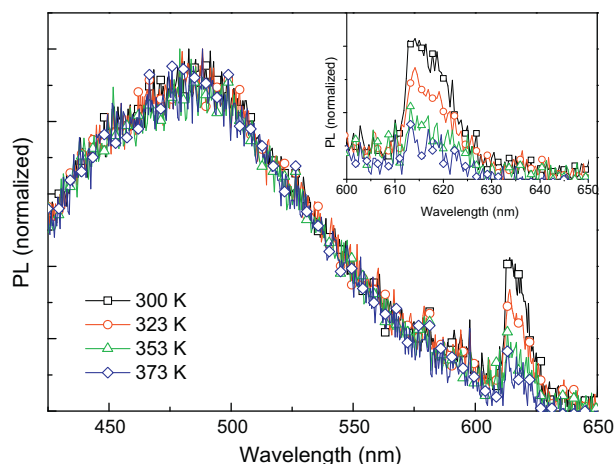


**Fig. 3.** (a) Comparison of two PL spectra before (filled squares) and after (empty squares) a complete heating-cooling cycle. (b) Ratio between two PL integrated areas: 600–625 nm ( $\text{Eu}^{3+}$  emission) and 440–460 nm (blue band). Solid line corresponds to a fit according to an Arrhenius type temperature dependence.

metal-to-ligand charge transfer state during copolymerization, often reported in copolymers containing lanthanide complexes [18], are ruled out here due to the removal of  $\text{Eu}^{3+}$  coordination, as discussed above.

The presence of a dual emission in the copolymer together with the different temperature dependent behaviour across the PL spectrum enables ratiometric determination of temperature as we will demonstrate below. Fig. 2a displays the PL spectra of copolymer slides at different temperatures under excitation at 380 nm. As temperature experiences a progressive rise from 298 K to 373 K, the  $\text{Eu}^{3+}$  emission becomes gradually weaker respect to the blue emission band. At 373 K the 613 nm emission peak is reduced by approximately 65% with respect to room temperature, (Fig. 2b). This change is almost completely reversible as demonstrated by the large degree of recovery after a complete heating-cooling cycle (Fig. 3a). The small hysteresis is most likely related to incomplete thermalization due to the slow heat dissipation during the cooling process.

We now address the origin of thermochromism in the copolymer. The relation between the ratio of emission at 612 nm and at 450 nm with temperature follows an Arrhenius type dependence  $I_{PL} \propto \exp(-\frac{E_a}{kT})$  with  $E_a$  the activation energy, (Fig. 3b). This result indicates that the mechanism leading to quenching of  $\text{Eu}^{3+}$  emission is thermally activated with activation energy of 0.12 eV estimated from the fit. We rule out thermal induced changes in population of singlets and triplets of the ligand as the origin of quenching since ligand absorption is negligible at 380 nm. On the other hand the energy offset between the emitting  $^5\text{D}_0$  electronic level and the immediate upper E atomic degeneracy is around



0.11 eV consistent with the value we found. [19] Thus we attribute the quenching of  $\text{Eu}^{3+}$  emission to thermal deactivation of the  $^5\text{D}_0$  population towards the upper E levels. Note that the selection rules restrict optical relaxation back to  $^5\text{D}_0$  thus leading to an effective emission quenching. This process is obviously reversible since a decrease in temperature leads to reduced thermal population of the E levels in favour of  $^5\text{D}_0$ . Accordingly, the ratio between the integrated PL both of 613 nm and the blue band upon excitation at 380 nm can be employed as the calibration curve for a molecular thermometer. Note that the strength of ratiometric measurements relies on the insensitivity to external factors, such as fluctuation in excitation intensity [20]. These latter are removed upon normalization by the second integrated PL band.

Furthermore, we attempted the integration of this sensing copolymer on a single index fibre based on PMMA by attaching a copolymer slide to one of the fibre tips. Upon excitation of the tip at 380 nm and detection at the opposed end of the fibre we observe both blue and  $\text{Eu}^{3+}$  emission (inset of Fig. 4). Compared with the emission from the block copolymer, the spectrum recorded at the end of the optical fibre displays some differences. The blue emission band is shifted from 450 nm to 490 nm. Most noticeable is the enhancement of intensity ratio between the blue band and the  $\text{Eu}^{3+}$  emission. Both differences are likely attributed to the characteristic attenuation of PMMA. A reduction of  $\text{Eu}^{3+}$  emission by almost 75% is observed at 373 K respect to room temperature.

This result suggests that the copolymer can be easily integrated in a POF preserving its temperature sensing functionalities. We tested different fibre lengths observing a strong attenuation of the blue band respect to  $\text{Eu}^{3+}$  emission as the fibre length increases.

#### 4. Conclusion

In conclusion we developed a new copolymer based on MMA and  $\text{Eu}(\text{dbm})_3\text{phen}$  which exhibits a large degree of reversible thermochromism. Ratiometric comparison of both  $\text{Eu}^{3+}$  peak and the residual emission ascribed to the organic ligands allows for univocal temperature determination. We demonstrate that this system can be easily integrated in POF fibres based in PMMA to allow for remote temperature sensing.

#### Acknowledgments

J. C-G acknowledges financial support from the Spanish Ministry of Science and Innovation through Programa Ramon y Cajal (RYC-2009-05475) and POLYDYE project (TEC2010-21830-C02-02). A.L.M acknowledges FCT-Portugal for a PhD grant.

#### References

- [1] J. Lee, N.A. Kotov, *Nanotoday* 2 (2007) 48.
- [2] C.M. Tan, J. Jia, W. Yu, *Appl. Phys. Lett.* 86 (2005) 263104.
- [3] J.J. Park, M. Taya, *J. Electron. Packaging* 128 (2006) 46.
- [4] H.Y. Chiu, W. Deshpande, H.W.C. Postma, C.N. Lau, C. Miko, L. Forro, M. Bockrath, *Phys. Rev. Lett.* 95 (2005) 226101.
- [5] S.M. Simon, *US Patent* 6 (2000) 132958.
- [6] M. Bruchez, M. Moronne, P. Gin, S. Weiss, P. Alivisatos, *Science* 281 (1998) 2013.
- [7] R. Levy, N.T.K. Thanh, R.C. Doty, I. Hussain, R.J. Nichols, D.J. Schiffrin, M. Brust, D.G. Fernig, *J. Am. Chem. Soc.* 126 (2004) 10076.
- [8] C.A. Mirkin, R.L. Letsinger, R.C. Mucic, J.J. Storhoff, *Nature* 382 (1996) 607.
- [9] C.M. Niemeyer, *Biochem. Soc. Trans.* 32 (2004) 51.
- [10] T. Mokari, E. Rothenberg, I. Popov, R. Costi, U. Banin, *Science* 304 (2004) 1787.
- [11] R. Melby, E. Abramson, J.C. Caris, N.J. Rose, *J. Am. Chem. Soc.* 86 (1964) 5117.
- [12] G.A. Crosby, R.E. Wham, R.M. Alire, *J. Chem. Phys.* 34 (1961) 743.
- [13] G.A. Crosby, *Mol. Cryst.* 1 (1966) 37.
- [14] H.G. Liu, Y.I. Lee, S. Park, K. Jang, S.S. Kim, *J. Lumin.* 110 (2004) 11.
- [15] M.D. McGehee, T. Bergstedt, C. Zhang, A.P. Saab, M.B. O'Regan, G.C. Bazan, V.I. Srdanov, A.J. Heeger, *Adv. Mater.* 11 (16) (1999) 1349.
- [16] L. Huang, L. Cheng, H. Yu, L. Zhou, J. Sun, H. Zhong, X. Li, J. Zhang, Y. Tian, Y. Zheng, T. Yu, J. Wang, B. Chen, *Physica B* 406 (2011) 2745.
- [17] M. Uekawa, Y. Miyamoto, H. Ikeda, K. Kaifu, T. Nakaya, *Bull. Chem. Soc. Jpn.* 71 (1998) 2253.
- [18] V. Bekiaris, P. Lianos, *Adv. Mater.* 17 (1998) 1455.
- [19] G.H. Dieke, *Spectra and Energy Levels of Rare Earth Ions in Crystals*, Interscience Publishers, New York, 1968.
- [20] J. Cabanillas-Gonzalez, O. Pena-Rodriguez, I.S. Lopez, M. Schmidt, M.I. Alonso, A.R. Goñi, M. Campoy-Quiles, *Appl. Phys. Lett.* 99 (2011) 103305.